KERNEL PRESERVING MULTIGRID METHODS FOR CONVECTION-DIFFUSION EQUATIONS

RANDOLPH E. BANK*, JUSTIN W. L. WAN†, AND ZHENPENG QU‡

Abstract. We propose a kernel preserving multigrid approach for solving convection-diffusion equations. The multigrid methods use Petrov-Galerkin coarse grid correction and linear interpolation. The restriction operator is constructed by preserving the kernel of the convection-diffusion operator. The construction considers constant and variable coefficient problems as well as cases where the convection term is not known explicitly. For constant convection-diffusion problems, we prove that the resulting Petrov-Galerkin coarse grid correction has small phase errors and the coarse grid matrix is almost an M-matrix. We demonstrate numerically the effectiveness of the multigrid methods by solving a constant convection problem, a recirculating flow problem and a real application problem for pricing Asian options.

Key words. Convection diffusion equations, multigrid, kernel preserving, interpolation, restriction

AMS subject classifications. 65D05, 65F10, 65F50, 65M12, 65M55

1. Introduction. We consider multigrid methods to solve convection diffusion equations of the form

$$-\nabla \cdot (\nabla u + \beta(x)u) = f, \qquad x \in \Omega,$$

where $\beta(x) \gg 1$. The equation can be discretized by upwinding finite difference methods [19], finite element methods [20] and finite volume methods [1]. In any case, the result is a linear system of the form

$$A^h u^h = f^h. \tag{1.1}$$

When $\beta(x) \equiv 0$, the linear system can be solved efficiently using, for instance, fast Fourier transform, preconditioned conjugate gradient, multigrid and domain decomposition methods. For large $\beta(x)$, however, A^h is a highly nonsymmetric matrix, and most of these solvers become less efficient.

Multigrid methods are widely used for solving elliptic partial differential equations (PDEs) because the convergence rates typically are independent of mesh size. For nonelliptic PDEs, in particular convection diffusion equations, multigrid convergence often deteriorates with increasing convection. One reason is that simple elliptic multigrid approaches do not take into account the hyperbolic nature of the convection diffusion operator. Thus modifications must be made in the smoother and coarse grid correction processes to improve convergence. Several smoothing techniques have been proposed to improve multigrid convergence. One approach is to apply Gauss-Seidel with the so-called downwind ordering [4, 7, 13, 18, 27]. Another approach is to use time-stepping schemes as smoothers for pure hyperbolic problems [15, 16, 17, 21].

*Department of Mathematics University of California, San Diego La Jolla, California 92093-0112. Email:rbank@ucsd.edu. The work of this author was supported by the National Science Foundation under contracts DMS-9973276 and DMS-0208449.

† School of Computer Science, University of Waterloo, Waterloo, ON, Canada N2L 3G1. Email: jwlwan@uwaterloo.ca. This author was supported by the Natural Sciences and Engineering Research Council of Canada.

‡ Department of Combinatorics and Optimization, University of Waterloo, Waterloo, ON, Canada N2L 3G1. Email: zqu@uwaterloo.ca. This author was supported by the Natural Sciences and Engineering Research Council of Canada.

Here the smoothers do not just reduce the high frequency errors, but also propagate the errors along the flow directions. The solution on the coarsest grid is typically done by a few smoothing steps. In this case, the multigrid process can be interpreted as speeding up the wave propagation by taking larger time step sizes on the coarse grids. As a result, errors can be removed rapidly by propagating them out of the boundary. Other possibilities include the use of line smoothers [22] or ILU smoothers [28, 29]. Although often effective, all these smoothers are relatively expensive to compute and apply, especially in three dimensions. Thus, in this paper, we primarily consider relaxation smoothers, and focus on the choice and construction of the interpolation and restriction operators.

Coarse grid correction leads to more subtle issues. Applying a first differential approximation (FDA) analysis and local mode analysis, one can show that for a model convection diffusion with constant coefficients, if the convection is not aligned with the grid and direct discretization is used to form the coarse grid matrix, the resulting two-level convergence factor is at best 0.5 [8]. The recent phase error analysis [25] leads to the same conclusion. These negative results pose the fundamental challenge of multigrid for solving convection diffusion equations.

One remedy is to apply artificial viscosity on the coarse grid matrices if the amount of viscosity can be determined a priori [33]. Another approach is to use Galerkin coarsening [32]. However, the Galerkin coarse grid matrices tend to central difference operators, leading to stability problems on coarse grids [12, 33]. In a recent analysis [30], it is shown that more accurate discrete coarse grid operators should be used for the direct discretization approach, and more accurate prolongation and restriction operators for the Galerkin approach. In another analysis [23], it is proved for a model problem that a Galerkin coarse grid matrix is an M-matrix for certain matrix-dependent interpolation. The Petrov-Galerkin approach has also been considered where the restriction and interpolation operators are allowed to be different. In [6, 31], different combinations of restriction (downstream residual transfer, full weighting) and interpolation (bilinear interpolation, upstream interpolation) operators are tested. In [10], the restriction and interpolation operators are constructed by applying the black box interpolation idea [9] to $(A^h)^T$ and the symmetric part of A^h, respectively. In [30], bilinear interpolation is also considered, but different restrictions are used for forming the coarse grid operator and performing the intergrid transfer.

In this paper, we consider the Petrov-Galerkin coarsening approach. We employ linear interpolation unless otherwise stated. The goal is to design a good restriction operator that exploits the hyperbolic nature of the PDEs, and is flexible enough to be applied on regular Cartesian grids as well as general unstructured grids. The latter is not addressed much in the approaches mentioned above. We also note that the construction of the interpolation and restriction operators in this paper is very related to the construction of approriate test and trial spaces in the hierarchical basis multigrid method [2, 3].

In Section 2, we describe the construction of our kernel preserving restriction operator. We first assume the convection $\beta(x)$ is known explicitly and then we generalize the kernel preserving restriction operator to the case when $\beta(x)$ is not given explicitly. In Section 3, we justify theoretically the importance of preserving the kernel in the construction of the restriction operator for the two-grid case. In particular, we prove that the coarse grid matrix is near an M-matrix and the phase error of the coarse grid correction process is negligibly small. In Section 4, we demonstrate the effectiveness of our multigrid methods by solving model problems as well as a real application

problem: Asian option pricing. We make some concluding remarks in Section 5.

2. Kernel preserving multigrid. For simplicity, we assume $\Omega = (0,1) \times (0,1)$ and the fine grid Ω^h is a regular triangular mesh with mesh size $h = 1/N$ and the grid point are given by

$$\{(x_i, y_j) : x_i = ih, y_j = jh, 0 \le i, j \le N\}.$$

Discrete functions $v^h = (v^h_{i,j})$ are grid functions defined on Ω^h. The discrete problem (1.1) is solved using K grids, $\{\Omega^l\}_{l=0}^{K-1}$, where the finest grid is Ω^{K-1}, and Ω^{l-1} is obtained from Ω^l by standard full coarsening [24]. Denote by P^l the interpolation (or prolongation) operator from Ω^{l-1} to Ω^l, and by R^l the restriction operator from Ω^l to Ω^{l-1}, $l = 1, 2, \ldots, K-1$. Also, denote the smoothing operator on Ω^l by $\mathcal{S}^l$. A standard multigrid V(q_1,q_2)-cycle algorithm [5, 12] consists of q_1 steps of pre-smoothing, q_2 steps of post-smoothing, and coarse grid corrections performed recursively on each coarse grid. On the coarsest grid, the discrete problem is solved exactly.

In this paper, we consider simple relaxation smoothers, e.g. damped Jacobi and Gauss-Seidel with natural ordering. We do not employ any special ordering in the smoothing, which can be quite complicated in general, especially in high dimensions. For coarse grid correction, we consider the Petrov-Galerkin approach, i.e. in the two-grid setting, the coarse grid operator is obtained from:

$$A^H = RA^hP,$$

where P and R are the interpolation and restriction operators, respectively, with $R \neq P^T$ in general. The focus of the paper is to construct P and R such that A^H is an accurate, and more importantly stable, approximation to A^h. Accuracy and stability issues will be made more precise in Section 3.

Our key idea for constructing P and R is to preserve the kernel of appropriate PDE operators. Specifically, we require the interpolation operator to preserve exactly certain kernel functions of the Laplace operator $\nabla \cdot \nabla$, namely constant and linear functions. A natural choice is linear interpolation and its construction is standard. For the restriction operator, we require it to preserve certain kernel functions of the convection-diffusion operator

$$\nabla \cdot (\nabla u + \beta u).$$

The details require further explanation. In the following, we discuss the construction of R, starting with simple cases, followed by more general situations.

2.1. Convection is known. When $\beta(x)$ is given analytically, conditions required to preserve the kernel functions are sufficient to determine the restriction operator when the fine mesh is obtained from regular refinement of a coarse triangular mesh. Here each noncoarse grid point is connected to precisely two coarse grid points.

2.1.1. Constant β. When $\beta(x)$ is constant, the kernel of the PDE operator

$$\nabla \cdot (\nabla u + \beta u)$$

consists of constant and exponential functions of the form

$$u(x) = \text{constant} \qquad \text{and} \qquad u(x) = e^{-\beta \cdot x}.$$

For simplicity, we describe the construction first in 1D.

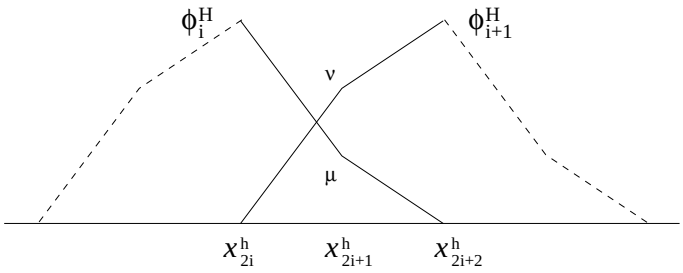

FIG. 2.1. *1D basis*

Consider the basis functions ϕ_i^H, ϕ_{i+1}^H as shown in Figure 2.1. Let $\mu = \phi_i^H(x_{2i+1}^h)$ and $\nu = \phi_{i+1}^H(x_{2i+1}^h)$. Thus, the stencil of the restriction operator is given by $[\nu \quad 1 \quad \mu]$. To determine μ and ν, we require ϕ_i^H and ϕ_{i+1}^H locally preserve the kernel exactly at x_{2i+1}^h. Specifically, for constant kernel functions, we require

$$\mu + \nu = 1. \tag{2.1}$$

For the exponential kernel functions, we require

$$e^{\beta h}\mu + e^{-\beta h}\nu = 1, \tag{2.2}$$

where h is the fine mesh size. Equations (2.1)-(2.2) can be easily solved as:

$$\mu = \frac{1}{1+e^{\beta h}}, \quad \nu = \frac{1}{1+e^{-\beta h}}. \tag{2.3}$$

These are the restriction weights for the multigrid algorithm. It is easy to construct once β is known. Note that when $\beta = 0$, i.e. pure diffusion, we recover full-weighting restriction (i.e. transpose of the linear interpolation). When β is large, however, it becomes an upwind biased piecewise constant restriction. One may view this as a generalization of the full-weighting restriction to convection-diffusion equations. We remark that the interpolation weights given in (2.3) have also been considered in [3] for constant coefficient PDEs. In this paper, we explore this idea further for the case where the PDE coefficients are not constants or even unspecified (and hence the kernel functions are not known), and the case where some of the noncoarse grid points are connected to more than 2 coarse grid points.

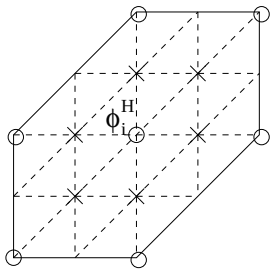

FIG. 2.2. *The support of a 2D coarse basis on a triangular grid. The circles denote the coarse grid connections and the crosses the noncoarse grid connections.*

In two dimensions (and similarly in higher dimensions), consider a generic coarse grid basis function ϕ_i^H defined on a standard uniform triangulation of a square domain

as shown in Figure 2.2. Circles indicate coarse grid points and crosses fine grid points. We compute the restriction weights at the noncoarse grid points in the same manner as in the one dimensional case and hence the derivation is omitted here. The resulting 7-point stencil of the restriction operator is then given by

$$\begin{bmatrix} 0 & \frac{1}{1+e^{-\beta\cdot(0,h)}} & \frac{1}{1+e^{-\beta\cdot(h,h)}} \\ \frac{1}{1+e^{-\beta\cdot(-h,0)}} & 1 & \frac{1}{1+e^{-\beta\cdot(h,0)}} \\ \frac{1}{1+e^{-\beta\cdot(-h,-h)}} & \frac{1}{1+e^{-\beta\cdot(0,-h)}} & 0 \end{bmatrix}. \tag{2.4}$$

As in the one-dimensional case, when $\beta = 0$, (2.4) reduces to linear restriction on triangular grids, as desired. When β is large, it becomes upwind biased piecewise constant restriction.

Remark: If the Cartesian grid is used instead, together with standard coarsening, then some of the noncoarse grid points will be connected to four coarse grid points. Thus, the above construction will fail. See Section 2.2 for the general case.

2.1.2. Variable β. The analytic form of the kernel of the convection term with variable coefficients is unknown in general. However, since restriction is a local process, we approximate the convection coefficient $\beta(x)$ locally by a constant. One approach is to pick the value of $\beta(x)$ at the noncoarse grid point and then apply the previous restriction. Specifically, consider Figure 2.3(a) which shows two generic coarse grid points in two dimensions. Let β be the value of the convection at $x_{2i+1,2j}$, i.e.

$$\beta = \beta(x_{2i+1,2j}). \tag{2.5}$$

Then, the restriction weights are given by the formula in (2.4).

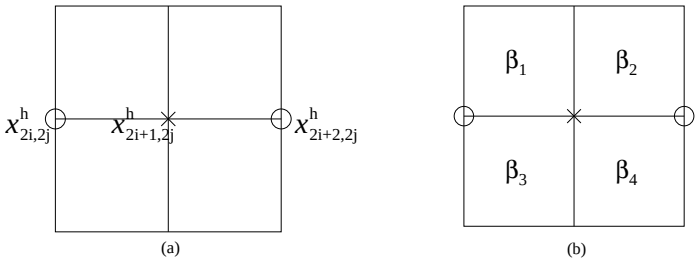

FIG. 2.3. *(a) Coarse connection of a noncoarse grid point at $x_{2i+1,2j}$. (b) Values of $\beta(x)$ near a noncoarse grid point.*

One may consider averaging the nearby values of $\beta(x)$. Consider Figure 2.3(b). We can define β as

$$\beta = \frac{\beta_1 + \beta_2 + \beta_3 + \beta_4}{4}. \tag{2.6}$$

The numerical results in Section 4 show that these two approaches lead to essentially the same multigrid convergence.

Another approach is to preserve the exponential kernel function $e^{-\beta\cdot x}$ for nonconstant β locally. Although it is no longer in the kernel of the variable coefficient PDE it remains a good local approximation. Let μ and ν be the restriction weights from the left and right coarse grid points, respectively, and let β_W, β_E and β_M be

the corresponding values of $\beta(x)$ at the two coarse grid points (x_W, x_E) and at the noncoarse grid point (x_M) in between. As in the one dimensional case, we impose two constraints as follows:

$$\mu + \nu = 1$$
$$e^{-\beta_W \cdot x_W}\mu + e^{-\beta_E \cdot x_E}\nu = e^{-\beta_M \cdot x_M}.$$

After some simple calculations, we obtain the restriction weights

$$\mu = \frac{e^{-\beta_M \cdot x_M} - e^{-\beta_E \cdot x_E}}{e^{-\beta_W \cdot x_W} - e^{-\beta_E \cdot x_E}}, \qquad \nu = \frac{e^{-\beta_W \cdot x_W} - e^{-\beta_M \cdot x_M}}{e^{-\beta_W \cdot x_W} - e^{-\beta_E \cdot x_E}}. \tag{2.7}$$

The coordinates of the grid points are also used in this case. It is noted that the weights in (2.7) equal those in (2.4) in the case of $\beta_M = \beta_W = \beta_E$.

2.2. Convection not known. In the previous section, the construction of the restriction operators made use of the explicit knowledge of $\beta(x)$; more precisely, the values of β at the grid points. While many applications provide such information, there are also situations where this information is not easily available. Furthermore, all these constructions assume the noncoarse grid points are connected to precisely two coarse grid points, which is hardly the case for unstructured grids, for example. In this section, we describe an algebraic approach that requires only the discretization matrix, and exploits the elliptic and hyperbolic aspects of the PDE via an energy minimization formulation.

2.2.1. Constant β. For the moment, assume the convection is constant and known, so the kernel of the convection operator is also known. Eventually β is not needed, but here we treat it as known to explain how a constrained minimization is formulated as described below. Now, however, we allow noncoarse grid points to have more than two coarse connections. As a result, there may be more degrees of freedom than constraints preserving the kernel functions. We formulate a minimization problem to select the "optimal" choice of restriction weights. The formulation is motivated by the elliptic PDE case. For elliptic PDEs, the energy minimization approach [26] defines an interpolation by utilizing coarse grid basis functions which satisfy

$$\min_{\phi_i^H \in V^H} \quad \sum_{i=1}^{M} \|\phi_i^H\|_A^2$$
$$\text{subject to} \quad \sum_{i=1}^{M} \phi_i^H(x_j^h) = 1 \qquad j = 1, \ldots, N,$$

where $\|\cdot\|_A$ is the energy norm associated with the matrix A, and V^H consists of piecewise linear functions $v^H(x)$ such that $v^H(x_i) = 1$ and $v^H(x_j) = 0$ if x_j is not a neighboring node of x_i. The idea of the energy minimization approach is based on the classical convergence theory of multigrid, which requires the interpolation to have stability and approximation properties. The minimal energy norm of the coarse grid basis is used to satisfy the stability property whereas the constant preserving constraint is used for the approximation property. Then an interpolation operator can be constructed from $\{\phi_i^H\}$. The resulting multigrid method has been shown to be robust and efficient, and its convergence is independent of the grid size h and the size of jumps in the PDE coefficients for a wide variety of elliptic problems [26].

Unfortunately, the convergence theory of multigrid for convection diffusion equations is not as well established. Nevertheless, we generalize the energy minimization formulation to convection dominated problems by a joint minimization formulation. Let $\{\phi_i^H\}$ and $\{\psi_i^H\}$ be the coarse grid basis functions corresponding to interpolation and restriction, respectively. Our approach is to compute $\{\phi_i^H\}$ and $\{\psi_i^H\}$ at the same time using the minimization problem

$$\min \quad \sum_{i=1}^{M} (\psi_i^H, \phi_i^H)_A \tag{2.8}$$

$$\text{subject to} \quad \begin{cases} \sum_{i=1}^{M} \phi_i^H(x_j^h) = 1 & \\ \sum_{i=1}^{M} e^{-\beta \cdot x_i^H} \psi_i^H(x_j^h) = e^{-\beta \cdot x_j^h} & j = 1, \ldots, N. \end{cases}$$

The operator $(\cdot,\cdot)_A$ is defined as follows. Let the vector representation of ψ_i^H and ϕ_i^H be $\phi^i = (\phi_1^i, \ldots, \phi_N^i)$ and $\psi^i = (\psi_1^i, \ldots, \psi_N^i)$, respectively. Then

$$(\psi_i^H, \phi_i^H)_A \equiv (\psi^i)^T A^h \phi^i.$$

Remarks:

1. When $\beta = 0$, A^h becomes the standard Laplace operator and is symmetric positive definite. Then $\{\psi_i^H\} = \{\phi_i^H\}$ and $(\psi_i^H, \phi_i^H)_A = \|\phi_i^H\|_A^2$, and hence reduces to the elliptic formulation. Thus, the new formulation (2.8) generalizes the energy minimization approach to the convection diffusion case.
2. The formulation has no assumptions on the geometry or dimension. So, it can be directly applied to problems defined on unstructured grids in any dimension.
3. In one dimension, the restriction operator constructed from $\{\psi_i^H\}$ is identical to the formula given in (2.3). However, the interpolation operator constructed from $\{\phi_i^H\}$ is not linear interpolation; in fact, it coincides with the restriction operator. As shown in Section 4, although the multigrid convergence is somewhat slower than that for linear interpolation, it does show mesh and convection independent convergence. We note, however, that one may simply use linear interpolation and disregard the one constructed from $\{\phi_i^H\}$.
4. In two dimensions, even the restriction is different from the formula given in (2.4) where only the kernel preserving is used. The interpolation is different from the restriction and it resembles a downwind piecewise constant interpolation for large β.

2.2.2. Nonconstant β. For variable and unspecified β, the kernel is not known analytically. Moreover we cannot use local values of $\beta(x)$ to approximate the kernel as $\beta(x)$ is not known explicitly, either. Our approach is based on the observation that the kernel of the PDE is related closely to the zero eigenvectors of the stiffness matrix. (Note that we do not need the stiffness matrix in our algorithm.) More precisely, the right zero eigenvector corresponds to the constant null space and the left zero eigenvector corresponds to the exponential kernel functions. Thus, we want the interpolation to preserve the right zero eigenvector and the restriction to preserve the left zero eigenvector. For standard finite difference or finite element discretizations, the right zero eigenvector of the discretization matrix is a vector of all 1's. Thus, it is consistent with the first constraint in our minimization formulation (2.8).

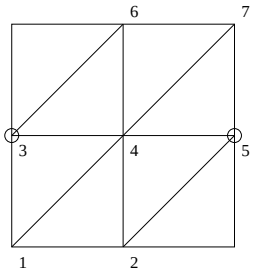

FIG. 2.4. *Extraction of a local matrix at the noncoarse grid point 4 for the computation of left and right zero eigenvectors.*

However, the left zero eigenvector is generally unknown, so we approximate it locally. Consider Figure 2.4 and in particular, the noncoarse grid point 4. For a 7-point stencil matrix, we extract the local 7×7 submatrix corresponding to the neighbors of point 4. (For a 9-point stencil matrix, the submatrix will be of size 9×9.) Replace the diagonal of the local matrix by the negative of the sum of the off-diagonal entries. The resulting matrix then resembles an element stiffness matrix.

Now compute the left and right zero eigenvectors of the local submatrix. Let $v^L = (v_1^L, \ldots, v_7^L)$ be the left zero eigenvector. To preserve this vector locally at grid point 4, we impose the constraint

$$v_3^L \mu + v_5^L \nu = v_4^L,$$

on the restriction weights μ, ν. This will be a constraint for the restriction operator. Similarly, the constraints for the interpolation operator can be set up using the right zero eigenvector. We note, however, that the right zero eigenvector is a constant vector and hence they need not be computed and the corresponding constraints are simply set to preserve the constant 1.

We remark that for constant β, the left zero eigenvector coincides with the discrete exponential kernel function and hence the minimization problem reduces to (2.8). However, the restriction is different from those given by (2.4) and (2.7), as mentioned in Remark 4 in the previous section.

2.2.3. Solution to minimization problem. We assume $\beta(x)$ is constant in the following. The procedure can be easily modified to the general case. For each coarse grid point i, write the coarse grid basis for interpolation as $\phi_i^H = \sum_{j=1}^n \varphi_j^i \phi_j^h$ and let $\varphi^i = (\varphi_1^i, \ldots, \varphi_n^i)^T$. Similarly, we write the coarse grid basis for restriction as $\psi_i^H = \sum_{j=1}^n \psi_j^i \phi_j^h$ and $\psi^i = (\psi_1^i, \ldots, \psi_n^i)^T$. Because of compact support, they are sparse vectors. Let $\Phi = [\varphi^1; \cdots; \varphi^m]$ be an $mn \times 1$ vector obtained by concatenating all the φ's. Do the same for Ψ. Then, (2.8) can be written as the following equivalent discrete linear constrained minimization problem:

$$\begin{aligned} \min \quad & \Psi^T \mathcal{A}^h \Phi \\ \text{subject to} \quad & \begin{cases} B_\Phi^T \Phi = \mathbf{1} \\ B_\Psi^T \Psi = \mathbf{1}. \end{cases} \end{aligned} \tag{2.9}$$

The symbol $\mathbf{1}$ denotes a vector of all 1's. The $mn \times mn$ matrix $\mathcal{A}^h$ is block diagonal with each block equal to $\mathcal{A}_i^h$ which is defined as

$$(\mathcal{A}_i^h)_{kl} = \begin{cases} A_{kl}^h & \text{if } \varphi_k^i \neq 0 \text{ and } \varphi_l^i \neq 0. \\ \delta_{kl} & \text{otherwise.} \end{cases}$$

The $n \times mn$ rectangular matrix $B_\Phi^T = [J_1 \cdots J_m]$ is defined as follows. J_i is a matrix corresponding to the injection operator that maps a vector v to v_i such that $(v_i)_k = (v)_k$ on $\mathrm{supp}(\phi_i^H)$ and $(v_i)_k = 0$ otherwise. More precisely,

$$(J_i)_{kl} = \begin{cases} 1 & \text{if } k = l \text{ and } \varphi_k^i \neq 0 \\ 0 & \text{otherwise.} \end{cases}$$

The $n \times mn$ rectangular matrix $B_\Psi^T = [K_1 \cdots K_m]$ is defined similarly, where

$$(K_i)_{kl} = \begin{cases} e^{-\beta \cdot (x_k^h - x_i^H)} & \text{if } k = l \text{ and } \psi_k^i \neq 0 \\ 0 & \text{otherwise.} \end{cases}$$

Now, we solve the discrete linear constrained minimization problem (2.9) by the Lagrange multiplier formulation, which is equivalent to

$$\begin{bmatrix} \mathcal{A}^T & 0 & B_\Phi & 0 \\ 0 & \mathcal{A} & 0 & B_\Psi \\ B_\Psi^T & 0 & 0 & 0 \\ 0 & B_\Phi^T & 0 & 0 \end{bmatrix} \begin{bmatrix} \Psi \\ \Phi \\ \Lambda_\Phi \\ \Lambda_\Psi \end{bmatrix} = \begin{bmatrix} \mathbf{0} \\ \mathbf{0} \\ \mathbf{1} \\ \mathbf{1} \end{bmatrix} \tag{2.10}$$

where Λ_Φ and Λ_Ψ are $n \times 1$ vectors of the Lagrange multipliers. By eliminating Φ and Ψ from (2.10), we obtain the equations for Λ_Φ and Λ_Ψ:

$$(B_\Psi^T \mathcal{A}^{-T} B_\Phi)\Lambda_\Phi = -\mathbf{1}$$
$$(B_\Phi^T \mathcal{A}^{-1} B_\Psi)\Lambda_\Psi = -\mathbf{1}$$

Note that B_Φ, B_Ψ, and $\mathcal{A}^{-1}$ are sparse matrices. We can solve the linear systems by a Krylov subspace method, e.g. BiCGStab.

Once Λ_Φ, Λ_Ψ are known, Φ and Ψ can be computed by solving

$$\mathcal{A}\Phi = -B_\Psi \Lambda_\Psi$$
$$\mathcal{A}^T \Psi = -B_\Phi \Lambda_\Phi.$$

Since $\mathcal{A}$ is block diagonal and inverting each block corresponds to solving a small matrix (e.g. the matrix size is 7×7 for a 7-point stencil matrix), it is straightforward to compute Φ and Ψ.

3. Theoretical justification. It is well known that if direct discretization is used as the coarse grid operator, the convergence rate of multigrid can be very poor. One reason is that the phase error can be relatively large. If the Galerkin coarse grid operator is used instead, the phase error is significantly smaller. However, it is known that Galerkin coarse grid operators can be unstable on coarse grids [12, 33]. In this section, we prove that the Petrov-Galerkin coarse grid operator has small phase error and is stable on the coarse grid.

In the following analysis, we assume the velocity $\beta(x)$ is the constant vector (β, β) so that it is not aligned with the computational grid. Also, the convergence rate of multigrid is usually poorest when the direction of the flow is at 45 degrees with the x-axis. Periodic boundary conditions are used, and we only consider two-grid analysis for the schemes described in Section 2.1. Although the algorithm is applicable to matrices arising from different discretization methods, in the following analysis, we consider primarily the Scharfetter-Gummel method [1]. We remark that unlike some

other discretization methods such as Streamline-Upwinding Petrov-Galerkin [14], the Scharfetter-Gummel discretization gives rise to an M-matrix if the triangulation is a Delaunay triangulation. The M-matrix property is of particular interest since it will guarantee nonoscillatory numerical solutions. Given that $\beta(x) = (\beta, \beta)$, the 5-point stencil of the Scharfetter-Gummel discretization matrix is given by:

$$\begin{bmatrix} & -\mathcal{B}(-\beta h) & \\ -\mathcal{B}(\beta h) & d & -\mathcal{B}(-\beta h) \\ & -\mathcal{B}(\beta h) & \end{bmatrix},$$

where $\mathcal{B}(x)$ is the Bernoulli function, defined as $\mathcal{B}(x) = x/(e^x - 1)$, and $d = 2\mathcal{B}(\beta h) + 2\mathcal{B}(-\beta h)$.

3.1. Phase error analysis. In [25], it was shown that the phase error of the coarse grid correction process is useful in determining the convergence rate of the corresponding multigrid method. It was proved that coarse grid matrices obtained from direct discretization lead to large phase errors whereas the Galerkin coarse grid matrices lead to significantly smaller phase errors. In the following, we show that the phase error of the Petrov-Galerkin coarse grid matrix is also small.

The phase error analysis is based on a Fourier analysis of a two-grid method. Let the discrete Fourier function, $\psi^h_{\mu,\nu}$, be written as

$$\psi^h_{\mu,\nu}(x^h_{j,k}) = \frac{1}{2} e^{i\mu\pi x^h_j} e^{i\nu\pi y^h_k} \qquad -N \le \mu, \nu \le N-1.$$

Thus, $\psi^h_{\mu,\nu}$, with $|\mu|$, $|\nu| \approx 0$, correspond to smooth or less oscillatory (low) modes whereas $\psi^h_{\mu,\nu}$, $|\mu|$, $|\nu| \approx N$, correspond to the most oscillatory (high) modes. For two-grid analysis, it is customary to pair up the low-low, high-low, low-high, and high-high modes together and hence the Fourier transform matrix Q_h is given by:

$$Q_h = [\cdots \psi^h_{\mu,\nu}\ \psi^h_{\mu,\nu'}\ \psi^h_{\mu',\nu}\ \psi^h_{\mu',\nu'} \cdots],$$

where $\mu' = \mu - N$, $\nu' = \nu - N$. Denote the Fourier transform of a matrix B by $\hat{B} \equiv Q_h^{-1} B Q_h$, with entries $\hat{B}_{\mu,\nu}$. In multigrid literature, $\hat{B}_{\mu,\nu}$ is often referred to the Fourier symbol of B.

The iteration matrix of the V(q_1,q_2)-cycle can be written as:

$$M = S^{q_2} C S^{q_1},$$

where C and S are coarse grid correction matrix and the iteration matrix of the smoother, respectively. Then $\hat{M} = \hat{S}^{q_2} \hat{C} \hat{S}^{q_1}$ is a block diagonal matrix with each block a 4×4 matrix $\hat{M}_{\mu,\nu}$ where

$$\hat{M}_{\mu,\nu} = \hat{S}^{q_2}_{\mu,\nu} \hat{C}_{\mu,\nu} \hat{S}^{q_1}_{\mu,\nu} \qquad \mu, \nu = -N/2, \ldots, N/2 - 1.$$

Hence the convergence rate is determined by the spectral radii of $\hat{M}_{\mu,\nu}$ which in turn depend on

$$\hat{C}_{\mu,\nu} = I - \hat{P}_{\mu,\nu} (\hat{A}^H_{\mu,\nu})^{-1} \hat{R}_{\mu,\nu} \hat{A}^h_{\mu,\nu},$$

where P, R and A^H are the prolongation, restriction and coarse grid operators, respectively. In phase error analysis, one assumes the smoothers are effective reducing

high frequency errors. Thus, $\hat{S}_{\mu,\nu}(1,1)$, the (1,1) entry of $\hat{S}_{\mu,\nu}$, is dorminant and the other entries are either zero or negligible. Consequenty, $\hat{M}_{\mu,\nu}$ is essentially determined by $\hat{C}_{\mu,\nu}(1,1)$, which represents the low frequency-low frequency interaction. In other words, it represents how the smooth waves are changed by the coarse grid correction. In theory, the ideal case is $\hat{C}_{\mu,\nu}(1,1)=0$. In general, $\hat{C}_{\mu,\nu}(1,1)$ is a nonzero complex number. The phase error analysis is to analyze how $\hat{C}_{\mu,\nu}(1,1)$, in particular, the phase angle of $\hat{C}_{\mu,\nu}(1,1)$, deviates from 0.

To analyze $\hat{C}_{\mu,\nu}(1,1)$, one first needs to compute the Fourier symbols $\hat{A}^h_{\mu,\nu}$, $\hat{A}^H_{\mu,\nu}$, $\hat{P}_{\mu,nu}$, and $\hat{R}_{\mu,\nu}$.

LEMMA 3.1. *The symbols of $\hat{A}^h$, $\hat{A}^H$, $\hat{P}$, $\hat{R}$ are given by*

$$\hat{A}^h_{\mu,\nu} = diag\left(\begin{bmatrix} \frac{\beta h}{1-e^{\beta h}}(e^{-\mu\pi hi}+e^{\beta h}e^{\mu\pi hi}+e^{-\nu\pi hi}+e^{\beta h}e^{\nu\pi hi}-2-2e^{\beta h}) \\ \frac{\beta h}{1-e^{\beta h}}(e^{-\mu\pi hi}+e^{\beta h}e^{\mu\pi hi}-e^{-\nu\pi hi}-e^{\beta h}e^{\nu\pi hi}-2-2e^{\beta h}) \\ \frac{\beta h}{1-e^{\beta h}}(-e^{-\mu\pi hi}-e^{\beta h}e^{\mu\pi hi}+e^{-\nu\pi hi}+e^{\beta h}e^{\nu\pi hi}-2-2e^{\beta h}) \\ \frac{-\beta h}{1-e^{\beta h}}(e^{-\mu\pi hi}+e^{\beta h}e^{\mu\pi hi}+e^{-\nu\pi hi}+e^{\beta h}e^{\nu\pi hi}-2-2e^{\beta h}) \end{bmatrix}\right)$$

$$\begin{aligned}\hat{A}^H_{\mu,\nu} = \frac{1}{4}\Bigg[&\frac{b}{2}\frac{\omega^2+\omega+2}{\omega^2+1}e^{-2\mu\pi hi}+\frac{a}{2}\frac{2\omega^2+\omega+1}{\omega^2+1}e^{2\mu\pi hi}\\ &+\frac{b}{2}\frac{\omega^2+\omega+2}{\omega^2+1}e^{-2\nu\pi hi}+\frac{a}{2}\frac{2\omega^2+\omega+1}{\omega^2+1}e^{2\nu\pi hi}\\ &+\frac{b(1-\omega)}{(\omega+1)(\omega^2+1)}e^{-2\mu\pi hi}e^{-2\nu\pi hi}+\frac{\omega^2(\omega-1)a}{(\omega+1)(\omega^2+1)}e^{2\mu\pi hi}e^{2\nu\pi hi}\\ &-b\frac{\omega^2+\omega+2}{\omega^2+1}-a\frac{2\omega^2+\omega+1}{\omega^2+1}-b\frac{1-\omega}{(\omega+1)(\omega^2+1)}-a\frac{\omega^2(\omega-1)}{(\omega+1)(\omega^2+1)}\Bigg]\end{aligned}$$

$$\hat{P}_{\mu,\nu} = \begin{bmatrix} c^2_\mu c^2_\nu \\ -s^2_\mu c^2_\nu \\ -c^2_\mu s^2_\nu \\ s^2_\mu s^2_\nu \end{bmatrix}$$

$$\hat{R}^T_{\mu,\nu} = \frac{1}{4}\begin{bmatrix} \frac{1}{1+e^{\beta h}}(e^{-\mu\pi hi}+e^{\beta h}e^{\mu\pi hi}+e^{-\nu\pi hi}+e^{\beta h}e^{\nu\pi hi})+\frac{1}{1+e^{2\beta h}}(e^{-(\mu+\nu)\pi hi}+e^{\beta h}e^{(\mu+\nu)\pi hi})+1 \\ \frac{1}{1+e^{\beta h}}(e^{-\mu\pi hi}+e^{\beta h}e^{\mu\pi hi}-e^{-\nu\pi hi}-e^{\beta h}e^{\nu\pi hi})+\frac{1}{1+e^{2\beta h}}(e^{-(\mu+\nu)\pi hi}+e^{\beta h}e^{(\mu+\nu)\pi hi})+1 \\ \frac{1}{1+e^{\beta h}}(-e^{-\mu\pi hi}-e^{\beta h}e^{\mu\pi hi}+e^{-\nu\pi hi}+e^{\beta h}e^{\nu\pi hi})+\frac{1}{1+e^{2\beta h}}(e^{-(\mu+\nu)\pi hi}+e^{\beta h}e^{(\mu+\nu)\pi hi})+1 \\ \frac{-1}{1+e^{\beta h}}(e^{-\mu\pi hi}+e^{\beta h}e^{\mu\pi hi}+e^{-\nu\pi hi}+e^{\beta h}e^{\nu\pi hi})+\frac{1}{1+e^{2\beta h}}(e^{-(\mu+\nu)\pi hi}+e^{\beta h}e^{(\mu+\nu)\pi hi})+1 \end{bmatrix}$$

where $c_\mu = \cos(\mu\pi h/2)$, $s_\mu = \sin(\mu\pi h/2)$, $\omega = e^{\beta h}$, and diag(d) denotes a diagonal matrix whose diagonal is d.

Proof. The symbols are obtained by direct computation; the details are omitted. □

From Lemma 3.1, it is clear that

$$\begin{aligned}\hat{C}_{\mu,\nu}(1,1) = 1-c^2_\mu c^2_\nu\Bigg[&\frac{1}{1+e^{\beta h}}(e^{-\mu\pi hi}+e^{\beta h}e^{\mu\pi hi}+e^{-\nu\pi hi}+e^{\beta h}e^{\nu\pi hi})\\ &+\frac{1}{1+e^{2\beta h}}(e^{-(\mu+\nu)\pi hi}+e^{\beta h}e^{(\mu+\nu)\pi hi})+1\Bigg]\frac{\hat{A}_{\mu,\nu}(1,1)}{\hat{A}^H_{\mu,\nu}}.\end{aligned}$$

To gain more insight into the formula of $\hat{C}_{\mu,\nu}(1,1)$, we consider two special and yet important cases: the frequency components in the characteristic direction, i.e. (μ,ν) such that

$$\mu - \nu = 0,$$

and the cross-characteristic direction[1] [6, 8, 30], i.e. (μ,ν) such that

$$\mu + \nu = 0.$$

THEOREM 3.2. *For the components in the characteristic direction,*

$$\hat{C}_{\mu,\nu}(1,1) = 1 - c_\mu^4 + O(\mu\pi h)^2.$$

For the components in the cross-characteristic direction,

$$\hat{C}_{\mu,\nu}(1,1) = 1 - c_\mu^4.$$

Proof. We first consider the frequency components in the characteristic direction, i.e. $\nu = \mu$. Let $a = -\mathcal{B}(-\beta h)$ and $b = -\mathcal{B}(\beta h)$. By Lemma 3.1, we have

$$\begin{aligned}\hat{A}^h_{\mu,\mu}(1,1) &= 2be^{-\mu\pi hi} + 2\omega be^{\mu\pi hi} - 2b - 2\omega b \\ &= 2b(-\mu\pi hi - \frac{(\mu\pi h)^2}{2}) + 2\omega b(\mu\pi hi - \frac{(\mu\pi h)^2}{2}) + O(\mu\pi h)^3.\end{aligned}$$

Similarly, $\hat{A}^H_{\mu,\mu}$ can be written as

$$\begin{aligned}\hat{A}^H_{\mu,\mu} &= \frac{b}{4(\omega^2+1)}\Big[(\omega^2+\omega+2)e^{-2\mu\pi hi} + \omega(2\omega^2+\omega+1)e^{2\mu\pi hi} + \frac{1-\omega}{1+\omega}e^{-4\mu\pi hi} \\ &\quad + \frac{\omega^3(\omega-1)}{\omega+1}e^{4\mu\pi hi} - \frac{\omega^3+2\omega^2+2\omega+3}{\omega+1} - \frac{\omega(3(\omega^3+2\omega^2+2\omega+1)}{\omega+1}\Big] \\ &= \frac{b}{4(\omega^2+1)(\omega+1)}\big[(\omega+1)(\omega^2+\omega+2)(-2\mu\pi hi - 2(\mu\pi h)^2) \\ &\quad + \omega(\omega+1)(2\omega^2+\omega+1)(2\mu\pi hi - 2(\mu\pi h)^2) + (1-\omega)(-4\mu\pi hi - 8(\mu\pi h)^2) \\ &\quad + \omega^3(\omega-1)(4\mu\pi hi - 8(\mu\pi h)^2)\big] + O(\mu\pi h)^3 \\ &= \frac{-\mu\pi hb}{(\omega^2+1)(\omega+1)}\big[(\omega+1)((1-\omega^3)i + (\omega^3+\omega^2+\omega+1)(\mu\pi h)) \\ &\quad + (1-\omega)((\omega^3+1)i + 2(1-\omega^3)(\mu\pi h)\big] + O(\mu\pi h)^3 \\ &= \frac{-\mu\pi hb}{(\omega^2+1)(\omega+1)}\big[2(1-\omega^4)i + (3\omega^4+2\omega^2+3)(\mu\pi h)\big] + O(\mu\pi h)^3.\end{aligned}$$

Combining these two formulae, we have

$$\begin{aligned}\frac{\hat{A}^h_{\mu,\mu}(1,1)}{\hat{A}^H_{\mu,\mu}} &= \frac{2(\omega+1)(\omega^2+1)(i+\frac{\mu\pi h}{2}) + 2\omega(\omega+1)(\omega^2+1)(-i+\frac{\mu\pi h}{2})}{2(1-\omega^4)i + (3\omega^4+2\omega^2+3)(\mu\pi h)} + O(\mu\pi h)^2 \\ &= 1 - \frac{\omega^3-1}{(\omega+1)(\omega^2+1)}\mu\pi hi + O(\mu\pi h)^2.\end{aligned}$$

[1] These components are also called characteristic components in the literature.

We then make a Taylor expansion of $\hat{R}_{\mu,\mu}(1,1)$ and obtain

$$\hat{R}_{\mu,\mu}(1,1) = 1 + \frac{\omega^3 - 1}{(\omega+1)(\omega^2+1)}\mu\pi hi + O(\mu\pi h)^2. \tag{3.1}$$

Finally,

$$\begin{aligned}\hat{C}_{\mu,\mu}(1,1) &= 1 - c_\mu^4 \left(1 + \frac{\omega^3-1}{(\omega+1)(\omega^2+1)}\mu\pi hi\right)\left(1 - \frac{\omega^3-1}{(\omega+1)(\omega^2+1)}\mu\pi hi\right) + O(\mu\pi h)^2 \\ &= 1 - c_\mu^4 + O(\mu\pi h)^2.\end{aligned}$$

In the cross-characteristic direction where $\nu = -\mu$,

$$\begin{aligned}\hat{A}^h_{\mu,-\mu}(1,1) &= -b(2 - e^{-\mu\pi hi} - \omega e^{-\mu\pi hi} - e^{\mu\pi hi} - \omega e^{\mu\pi hi} + 2\omega) \\ &= -2b(\omega+1)(1-\cos(\mu\pi h)) \\ &= -4b(\omega+1)s_\mu^2.\end{aligned}$$

Similarly,

$$\begin{aligned}\hat{A}^H_{\mu,-\mu} &= \frac{b}{8(\omega^2+1)}(\omega^2+\omega+2+2\omega^3+\omega^2+\omega)(e^{-2\mu\pi hi} + e^{2\mu\pi hi} - 2) \\ &= \frac{-b(\omega^3+\omega^2+\omega+1)\sin^2(\mu\pi h)}{\omega^2+1}.\end{aligned}$$

For the restriction operator, we have

$$\hat{R}_{\mu,-\mu} = \frac{1}{4}\left(\frac{1}{\omega+1} + \frac{\omega}{\omega+1}\right)(e^{-\mu\pi hi} + e^{\mu\pi hi} + 2) = c_\mu^2.$$

Combining all the formulae, we obtain

$$\begin{aligned}\hat{C}_{\mu,-\mu}(1,1) &= 1 - c_\mu^6 \frac{-4b(\omega+1)s_\mu^2}{\frac{-b(\omega^3+\omega^2+\omega+1)\sin^2(\mu\pi h)}{\omega^2+1}} \\ &= 1 - c_\mu^6 \frac{4(\omega+1)(\omega^2+1)s_\mu^2}{(\omega^3+\omega^2+\omega+1)4s_\mu^2 c_\mu^2} \\ &= 1 - c_\mu^4.\end{aligned}$$

□

It is interesting to note that the phase error in the characteristic direction of the coarse grid matrix relative to the fine grid matrix can be quite significant. More precisely, for $\omega \to \infty$ (i.e. $\beta \to \infty$),

$$\frac{\hat{A}^h_{\mu,\nu}(1,1)}{\hat{A}^H_{\mu,\nu}} \approx 1 - \mu\pi hi + O(\mu\pi h)^2 = e^{-\mu\pi hi} + O(\mu\pi h)^2.$$

If one ignores the effect of prolongation and restriction, then the coarse grid correction has the effect of shifting waves of any frequency by 1 grid point to the right. For $\omega \to 0$ (i.e. $\beta \to -\infty$),

$$\frac{\hat{A}^h_{\mu,\nu}(1,1)}{\hat{A}^H_{\mu,\nu}} \approx e^{\mu\pi hi} + O(\mu\pi h)^2.$$

In this case, the convection has an opposite direction and the phase error has the effect of shifting waves by 1 grid point to the left. As a result, the coarse grid error is off by 1 grid point compared to the fine grid error, leading to at most first order accurate approximation. Fortunately, the restriction operator has the same but opposite effect, as can be seen by its symbol where the sign is positive for the term $\mu\pi hi$; see (3.1). It counteracts the shifting caused by the Petrov-Galerkin coarse grid matrix. As a result, one can easily derive from $\hat{C}_{\mu,\nu}(1,1)$ that the phase error of the Petrov-Galerkin coarse grid correction is only $O(\mu\pi h)^2$. For comparison, the phase errors of the direct discretization and Galerkin coarse grid correction approaches are $1/2$ and $O(\mu\pi h)^3$, respectively [25]. Although Petrov-Galerkin is not as accurate as the Galerkin approach, it is certainly much better than direct discretization. Moreover, in the cross-characteristic direction, $\hat{C}_{\mu,\nu}(1,1)$ is close to zero, in contrast with the direct discretization approach where $\hat{C}_{\mu,\nu}(1,1) = 1/2$ [8, 30] which leads to a convergence rate of at most 0.5.

The phase error of Petrov-Galerkin coarse grid correction is not as small as that of Galerkin coarse grid correction. However, Galerkin coarse grid operators are often not stable. In the next section, we shall show the stability of Petrov-Galerkin coarse grid operators.

3.2. M-matrix property. If the fine grid discretization matrix is an M-matrix, there will be no spurious oscillation in the numerical solution. For stability, it is desirable that the coarse grid matrix inherits the M-matrix property of the fine grid matrix. If direct discretization is used to construct the coarse grid matrix, it would clearly be an M-matrix, but then it leads to poor coarse grid correction and large phase errors. On the other hand, if Galerkin coarse grid matrix is used, it may not necessarily be an M-matrix.

Here, we prove that our Petrov-Galerkin coarse grid matrix with linear interpolation and exponential fitting restriction is almost an M-matrix. More precisely, it approaches to an M-matrix asymptotically as $|\beta|$ approaches infinity. We first compute the entries of the coarse grid matrix.

LEMMA 3.3. *Denote the stencil of the course grid matrix A^H by*

$$\begin{bmatrix} & A^H_N & A^H_{NE} \\ A^H_W & A^H_C & A^H_E \\ A^H_{SW} & A^H_S & \end{bmatrix},$$

where A^H is obtained by linear interpolation and exponential fitting restriction (2.4). Then

$$\begin{aligned} A^H_N &= \frac{2\omega^2+\omega+1}{2(\omega^2+1)}a, \quad & A^H_{NE} &= \frac{\omega^2(\omega-1)}{(\omega+1)(\omega^2+1)}a, \\ A^H_W &= \frac{\omega^2+\omega+2}{2(\omega^2+1)}b, \quad & A^H_E &= \frac{2\omega^2+\omega+1}{2(\omega^2+1)}a, \\ A^H_{SW} &= \frac{1-\omega}{(\omega+1)(\omega^2+1)}b, \quad & A^H_S &= \frac{\omega^2+\omega+2}{2(\omega^2+1)}b, \\ A^H_C &= -(A^H_N + A^H_{NE} + A^H_W + A^H_E + A^H_{SW} + A^H_S), \end{aligned}$$

where a, b, and ω are defined as before.

Proof. The computation of all the entries of A^H is similar so we only show the formula for A^H_W. Let I be the index of a coarse grid unknown and i be the index of the

corresponding unknown on the fine grid. Then $i = 2I$, assuming standard coarsening. Also, denote the number of fine grid points in the x-direction by nx. Let P and R be the linear interpolation and exponential fitting restriction operators, respectively. By the definition of the Petrov-Galerkin coarse grid matrix

$$\begin{aligned}
A^H_W = A^H_{I,I-1} &= (RA^hP)_{I,I-1} \\
&= \sum_i R_{I,i} \sum_j A^h_{i,j} P_{j,I-1} \\
&= \sum_i R_{I,i} \left[\frac{1}{2} A^h_{i,2I-nx-3} + \frac{1}{2} A^h_{i,2I-nx-2} + \frac{1}{2} A^h_{i,2I-3} + A^h_{i,2I-2} + \frac{1}{2} A^h_{i,2I-1} \right. \\
&\quad \left. + \frac{1}{2} A^h_{i,2I+nx-2} + \frac{1}{2} A^h_{i,2I+nx-1} \right] \\
&= \frac{1}{\omega^2+1} (\frac{1}{2} A^h_{2I-nx-1,2I-nx-2} + \frac{1}{2} A^h_{2I-nx-1,2I-1}) \\
&\quad + \frac{1}{\omega+1} (A^h_{2I-1,2I-2} + \frac{1}{2} A^h_{2I-1,2I-1} + \frac{1}{2} A^h_{2I-1,2I+nx-1}) \\
&\quad + \frac{1}{2} A^h_{2I,2I-1} + \frac{\omega}{\omega+1} (\frac{1}{2} A^h_{2I+nx,2I+nx-1}) \\
&= \frac{1}{\omega^2+1} (\frac{1}{2} b + \frac{1}{2} a) + \frac{1}{\omega+1} (b + \frac{1}{2}(-2a-2b) + \frac{1}{2} a) + \frac{1}{2} b + \frac{\omega}{\omega+1} (\frac{1}{2} b) \\
&= \frac{\omega(1-\omega)}{2(\omega^2+1)(\omega+1)} a + \frac{2\omega^3+\omega^2+3\omega+2}{2((\omega^2+1)(\omega+1)} b.
\end{aligned}$$

The result follows from the fact that $a = \beta h e^{\beta h}/(1-e^{\beta h}) = \omega b$. □

THEOREM 3.4. *The Petrov-Galerkin coarse grid matrix can be written as:*

$$A^H = \bar{A}^H + E^H,$$

where $\bar{A}^H$ is an M-matrix and $E^H = O(e^{-2|\beta|h})$ as $|\beta|$ approaches infinity.

Proof. Note that $a < 0$, $b < 0$, and $\omega \equiv e^{\beta h} > 0$. Thus, by Lemma 3.3, all of the off-diagonal entries of A^H are negative, except for A^H_{NE} and A^H_{SW}. Consider

$$A^H_{SW} = \frac{1-\omega}{(\omega+1)(\omega^2+1)} b.$$

If $\beta \leq 0$, then $\omega \leq 1$ and so $A^H_{SW} \leq 0$. If $\beta > 0$, however, then $A^H_{SW} > 0$. Similarly, for

$$A^H_{NE} = \frac{\omega^2(\omega-1)}{(\omega+1)(\omega^2+1)} a,$$

it is non-positive if $\beta \geq 0$ and positive if $\beta < 0$. Now, consider the case when $\beta \geq 0$. Let $\bar{A}^H$ have the same stencil as A^H with A^H_{SW} replaced by 0. Also, the diagonal entries of $\bar{A}^H$ are defined as the negative sum of the off-diagonal entries. Then it is clear that $\bar{A}^H$ is an M-matrix. For the other case when $\beta \leq 0$, we let $\bar{A}^H$ have the same stencil as A^H with A^H_{NE} replaced by 0. Then, again, $\bar{A}^H$ is an M-matrix. Furthermore, when $\beta \to \infty$,

$$A^H_{SW} \to \frac{-1}{\omega^2} b = O(e^{-2\beta h}).$$

When $\beta \to -\infty$,

$$A^H_{NE} \to -\omega^2 a = O(e^{2\beta h}).$$

Thus $E^H = A^H - \bar{A}^H = O(e^{-2|\beta|h})$. □

We note that A^H is not an M-matrix in exact arithmetic; however, the error term decays exponentially and becomes the order of roundoff error for sufficiently large β. So for convection dominated problems, we should expect numerically stable Petrov-Galerkin coarse grid matrices.

4. Numerical results. In this section, we present results of numerical experiments in two dimensions that demonstrate the effectiveness of the proposed multigrid methods. In all the numerical examples, the computational domain is $\Omega = [0,1] \times [0,1]$ with homogeneous Dirichlet boundary conditions. We discretize the PDE on a regular Cartesian mesh and finite difference (upwinding or otherwise stated) methods are used. In the multigrid procedure, a V-cycle is used with two pre- and two post-smoothings, unless stated otherwise. Damped Jacobi and Gauss-Seidel (GS) smoothers are considered. The coarse grid operators are obtained from Petrov-Galerkin coarsening with linear interpolation and restriction as specified in each example. Since some of the numerical results are compared with those reported in other papers, the stopping criterion varies. Typically, the iteration was terminated when the relative residual l_2-norm was less than 10^{-6} or 10^{-8}.

Example 1: In this example, we consider the following constant coefficient convection diffusion equation [10, example 1]:

$$-\delta h \Delta u + u_x + u_y = f.$$

In [10], the smoother used is Kaczmarz with one pre-smoothing and one post-smoothing. Linear interpolation is used together with restriction obtained from applying the black box interpolation [9] idea to A^T. The coarse grid operator is formed by Petrov-Galerkin. We used simple damped Jacobi as smoother. As the cost of one Kaczmarz iteration is approximately equal to two Jacobi iterations, the number of pre- and post-smoothings is two instead. We used linear interpolation, but exponential fitting restriction as defined in Section 2.1 and 2.2. The stopping criterion is 10^{-6}.

In order to compare with the results given in [10], we select $h = 1/32$ and vary δ. The convergence results are shown in Table 4.1. BMG denotes the black box multigrid and EMG denotes our multigrid method. The bracket specifies the smoother used. For relatively large δ, the two multigrid methods are comparable. However, as δ becomes smaller, the convergence of BMG deteriorates while EMG(Jac) remains efficient. In fact, EMG(Jac) shows somewhat better convergence for small δ. Hence, the kernel preserving restriction results in convection independent multigrid convergence.

Table 4.1 also shows the multigrid convergence results for Gauss-Seidel smoothers with different ordering. GS_1 denotes the ordering first in the x-direction (left to right) and then in the y-direction (bottom to top), which is just the natural ordering. GS_2 denotes the ordering first in the y-direction (top to bottom) and then x-direction (left to right). GS_3 denotes the ordering first in the x-direction (right to left) and then y-direction (top to bottom). Finally, GS_4 denotes the ordering first in the y-direction (bottom to top) and then x-direction (right to left). The results are generally worse than those for damped Jacobi smoothing, except for EMG(GS_1), where the ordering is consistent with the flow direction. The worst results are given by EMG(GS_3) whose

δ	BMG	EMG(Jac)	EMG(GS_1)	EMG(GS_2)	EMG(GS_3)	EMG(GS_4)
1	11	11	6	6	8	6
1/2	13	10	5	7	9	7
1/4	20	10	4	6	11	6
1/8	> 20	9	3	8	15	8
1/16	> 20	9	3	10	18	10

TABLE 4.1

Number of multigrid V-cycles for a convection diffusion equation with convection term $\beta(x) = -[1, 1]$ *and varying diffusion coefficient,* δh.

ordering is opposite to the flow direction. Thus, in contrast with diffusion dominated problems, Gauss-Seidel shows a poorer smoothing effect compared to damped Jacobi, but can still be an effective smoother if the ordering happens to be consistent with the flow direction.

We also tested our multigrid method by fixing the diffusion term, i.e. $\delta h = 10^{-3}$ and varying the mesh size. The results are shown in Table 4.2. EMG(Jac) and EMG(GS_1) perform the best and their convergence rates are independent of the mesh size, h. The convergence rates of other EMG methods are much slower and are generally dependent on the mesh size, similar to the results shown in Table 4.1. We also note that their convergence behavior is somewhat irregular with respect to the mesh size; they converge faster when $h = 1/128$ then when $h = 1/64$. It may be due to the poor smoothing effect.

h	EMG(Jac)	EMG(GS_1)	EMG(GS_2)	EMG(GS_3)	EMG(GS_4)
1/16	9	2	6	11	6
1/32	9	2	10	18	10
1/64	9	3	15	28	15
1/128	9	3	12	14	12

TABLE 4.2

Number of multigrid V(2,2)-cycles for a convection diffusion equation with convection term $\beta(x) = -[1, 1]$, *diffusion coefficient* $\delta h = 10^{-3}$, *and varying mesh size* h.

Example 2: We consider a variable coefficient problem, often known as the recirculating flow problem:

$$\epsilon \Delta u + a u_x + b u_y = f,$$

where $a = 4x(x-1)(1-2y)$, $b = -4y(y-1)(1-2x)$. In this case, the kernel of the PDE operator is unknown and so we use a locally defined value of $\beta(x)$ to construct the restriction, as described in Section 2.1.2. Denote the multigrid using the midpoint value of $\beta(x)$, (2.5), by $EMG(\beta_{midpt})$, the average of nearby values of $\beta(x)$, (2.6), by $EMG(\beta_{ave})$, and multigrid with restriction locally preserving $e^{-\beta \cdot x}$, (2.7), by $EMG(\beta_{weighted})$. In this example, we use GS with ordering depending on the sign of a and b; see [30]. Basically, we sweep over the variables four times in the appropriate order, and in each sweep relaxing roughly one quarter of the variables as follows: in the first sweep only variables at locations where both $a(x)$ and $b(x)$ are nonnegative are relaxed; in the second sweep only variables corresponding to locations where $a(x)$ is nonnegative and $b(x)$ is nonpositive are relaxed; and similarly for the third and fourth sweeps. ϵ is taken as 10^{-3}. The stopping criterion is 10^{-8}.

h	EMG(β_{midpt})	EMG(β_{ave})	EMG($\beta_{weighted}$)
1/16	6	6	4
1/32	7	7	6
1/64	10	10	8
1/128	12	12	10

TABLE 4.3

Number of multigrid V(2,1)-cycles for the recirculating flow problem. The multigrid methods obtained from different choices of β are compared.

Table 4.3 shows the number of V-cycles of different multigrid methods. The choices of using the local midpoint $\beta(x)$ and using the average of local values of $\beta(x)$ give rise to two multigrid methods with similar convergence. All these methods, however, show a small logarithmic dependence on the mesh size.

We also compare our results with the those of Yavneh [30], who developed an efficient multigrid method for solving the recirculating flow problems. He tested two types of coarse grid correction, non-Galerkin and Petrov-Galerkin. For the non-Galerkin approach, the coarse grid operator is obtained from two discretizations of different accuracy. He used the same GS smoothing as ours, V(2,1)-cycle, bilinear interpolation, and full-weighted restriction. For the Petrov-Galerkin approach, the coarse grid operator is obtained from a linear interpolation and a restriction operator such that the scheme remains "upstream on all grids". (Note: these operators are different from the intergrid transfer operators.) Artificial viscosity is also added to the coarse grid operator. The stopping criterion is 10^{-8}.

h	ϵ	EMG($\beta_{weighted}$)	EMG(β_{midpt})	Non-Galerkin	Petrov-Galerkin
1/64	∞	9	6	N/A	N/A
1/64	10^{-2}	11	8	N/A	N/A
1/64	10^{-3}	8	10	N/A	N/A
1/64	10^{-5}	8	11	N/A	N/A
1/128	∞	10	6	8	8
1/128	10^{-1}	10	6	8	8
1/128	10^{-3}	10	12	27	10
1/128	10^{-5}	10	12	19	13
1/128	10^{-7}	9	12	17	14
1/128	10^{-9}	9	12	N/A	N/A
1/256	∞	9	7	N/A	N/A
1/256	10^{-3}	10	12	N/A	N/A
1/256	10^{-5}	10	13	N/A	N/A
1/256	10^{-7}	10	13	24	12
1/256	10^{-9}	10	13	N/A	N/A

TABLE 4.4

Number of multigrid V(2,1)-cycles for the recirculating flow problem The multigrid methods are compared using different ϵ and mesh size h. The Non-Galerkin and Petrov-Galerkin columns show the multigrid results given in [30]. N/A denotes unavailable results.

The results are shown in Table 4.4 (N/A denotes results not available in [30]). First, we see that the iteration numbers of EMG are insensitive to mesh size and ϵ. EMG($\beta_{weighted}$) seems generally better than EMG(β_{midpt}) but the difference is

not very significant. The non-Galerkin approach discussed by Yavneh shows poorer convergence and stronger dependence on h and ϵ. The Galerkin approach discussed by Yavneh shows similar convergence behavior. However, the coarse grid operator is somewhat more complicated to construct and it is unclear how to construct the linear and restriction operators in general. Also, artificial viscosity was needed but it was not discussed how much one should add. For our multigrid approach, we use the same interpolation and restriction operators for both intergrid transfer and the construction of the coarse grid matrices. Also, we do not require artificial viscosity.

Example 3: We consider the same equation as in Example 1, but the multigrid method uses the restriction and interpolation operators constructed by solving the minimization problem described in Section 2.2.3. Both damped Jacobi and Gauss-Seidel smoothings are tested. The results are shown in Table 4.5.

h	EMG(Jac)	EMG(GS_1)	EMG(GS_2)	EMG(GS_3)	EMG(GS_4)
1/16	8	2	6	9	6
1/32	9	2	11	17	11
1/64	11	3	16	28	16
1/128	12	3	16	28	16

TABLE 4.5

Number of multigrid V(2,2)-cycles for a convection diffusion equation with convection term $\beta(x) = -[1, 1]$, diffusion coefficient $\delta h = 10^{-3}$, and varying mesh size h. The restriction and interpolation operators are constructed from solving a minimization problem.

This multigrid method does not take advantage of the Cartesian geometry and does not make explicit use of the knowledge of the convection term and hence it is completely algebraic. Since it is more general, it is not expected to be as efficient as the multigrid method considered in Example 1. The results shown in Table 4.5, however, are comparable to those in Table 4.2. EMG(Jac) here is a bit slower than in Example 1 and also shows a slight dependence on the mesh size. On the whole, nonetheless, there is no significant difference between the results of the two EMG approaches. It would be interesting to see the results of this general approach to solving more general problems, e.g. unstructured grids. This will be considered in the future research.

Example 4: We apply our EMG multigrid method to solve a real application problem: pricing Asian options. The price of an Asian option, V, can be found by solving a PDE in two dimensions based on the Black-Scholes equations:

$$\frac{\partial V}{\partial \tau} = \frac{1}{2}\sigma^2 S^2 \frac{\partial^2 V}{\partial S^2} + rS\frac{\partial V}{\partial S} + \frac{1}{T-\tau}(S-A)\frac{\partial V}{\partial A} - rV, \tag{4.1}$$

where S is the stock price, A is the arithmetic average of the stock price over some time interval T, τ is the time from the expiration date T, r and σ are constants representing the risk free interest rate and volatility. It is not within the scope of this paper to derive this equation; we refer the interested readers to [11, 34]. For fixed strike call options, the terminal boundary condition is:

$$V(S(T), A(T), T) = max(A(T) - K, 0),$$

where K is the strike price of an option. The boundary condition at $S = 0$ is:

$$\frac{\partial V}{\partial \tau} = \frac{-A}{T-\tau}\frac{\partial V}{\partial A} - rV.$$

For boundary condition at $S \to \infty$, we make the standard assumption that $\frac{\partial^2 V}{\partial S^2} \to 0$. The equation is discretized using an implicit finite volume method.

In each time step, one needs to solve the implicit equation corresponding to the convection diffusion equation (4.1). It is important to note that there is no diffusion in the A direction, which is the source of many numerical difficulties. It is a particularly interesting test case for multigrid since it is very convection dominated (in fact, pure hyperbolic) in the A direction and the convection is not constant. We apply our multigrid of Section 2.2.2 with point GS smoothing to solve the zero strike call option (i.e. $K = 0$), a case where the analytic solution is known. We used the same parameters as in [11] where $r = 0.1$ and the initial stock price is $S_0 = 100$. The mesh size $h = 1/64$ and the time step size $\Delta\tau = 0.025$. The stopping criterion is 10^{-6}.

σ	T	Analytic	Numerical	EMG(GS)
0.1	0.25	98.763	98.7604	12
0.1	0.50	97.547	97.5411	9
0.1	1.00	95.175	95.1626	6
0.2	0.25	98.763	98.7574	12
0.2	0.50	97.547	97.5309	9
0.2	1.00	95.175	95.1785	6
0.4	0.25	98.763	98.7673	12
0.4	0.50	97.547	97.5447	9
0.4	1.00	95.175	95.1633	6

TABLE 4.6

Analytical and numerical solution for an Asian call option with zero strike and the average number of multigrid V(2,2)-cycles over all time steps for solving the Asian option model equation.

Table 4.6 shows the numerical results with different practical values of σ, leading to different strength of diffusion. The numerical solutions are in good agreement with the analytic solutions. Moreover, our EMG method converges in between 6 to 12 multigrid iterations on the average in each time step. More precisely, the method consistently converges in about 3 iterations when τ is small and in about 16 iterations when τ approaches the final time T (strong convection). Thus, the average iteration numbers tend to be larger for T small and smaller for T large.

5. Conclusions. We have demonstrated that Petrov-Galerkin coarse grid correction together with linear interpolation and kernel preserving restriction will lead to a fast convergent multigrid method for solving convection-diffusion equations. The main reason is that the coarse grid correction process is accurate and stable. Although the coarse grid matrix has a phase error of $1/2$ which shifts waves of any frequency by one grid point, the kernel preserving restriction has the same but opposite effect that counteracts the shifting caused by the coarse grid matrix. As a result, the coarse grid correction is accurate. Moreover, we have proved that the Petrov-Galerkin coarse grid matrix is stable in the sense that it is asymptotically an M-matrix for large β.

We have also considered the general case where $\beta(x)$ is not given explicitly and proposed a joint minimization formulation to construct the restriction operator. The convergence rate of the resulting multigrid method has been shown to be comparable to that given by exponential fitting restriction. However, we note that one needs to solve a minimization problem which may be costly. The algorithms are implemented in MATLAB and so accurate timings for constructing the restriction operator are not

available. However, we refer the interested reader to [26] for more discussions on the cost of the minimization problem. This general approach is purely algebraic in nature and so it is applicable to complicated geometries such as unstructured grids, but these cases are not discussed in the present paper.

REFERENCES

[1] R. E. Bank, W. M. Coughran, and L. C. Cowsar. The finite volume Scharfetter-Gummel method for steady convection diffusion equations. *Comput. Visual. Sci.*, 1:123–136, 1998.

[2] R. E. Bank, T. F. Dupont, and H. Yserentant. The hierarchical basis multigrid method. *Numer. Math.*, 52:427–458, 1988.

[3] R. E. Bank and S. Gutsch. Hierarchical basis for the convection-diffusion equation on unstructured meshes. In P. Bjorstad, M. Espedal, and D. Keyes, editors, *Ninth International Conference on Domain Decomposition Methods*, pages 251–265. John Wiley & Son, 1998.

[4] J. Bey and G. Wittum. Downwind numbering: Robust multigrid for convection-diffusion problems. *Appl. Numer. Math.*, 23:177–192, 1997.

[5] A. Brandt. Multi-level adaptive solutions to boundary-value problems. *Math. Comp.*, 31:333–390, 1977.

[6] A. Brandt. Multigrid solvers for non-elliptic and singular-perturbation steady-state problems. Department of Applied Mathematics, The Weizmann Institute of Science, 76100 Rehovot, Israel, 1981.

[7] A. Brandt and I. Yavneh. On multigrid solution of high-Reynolds incompressible entering flows. *J. Comput. Phys.*, 101:151–164, 1992.

[8] A. Brandt and I. Yavneh. Accelerated multigrid convergence and high-Reynolds recirculating flows. *SIAM J. Sci. Comput.*, 14:607–626, 1993.

[9] J. E. Dendy, Jr. Black box multigrid. *J. Comp. Phys.*, 48:366–386, 1982.

[10] J. E. Dendy, Jr. Black box multigrid for nonsymmetric problems. *Appl. Math. Comput.*, 13:261–283, 1983.

[11] Y. d'Halluin, P. A. Forsyth, and G. Labahn. A semi-Lagrangian approach for American Asian options under jump diffusion. To appear in *SIAM J. Sci. Comput.*, 2004.

[12] W. Hackbusch. *Multi-grid Methods and Applications.* Springer-Verlag, Berlin, 1985.

[13] W. Hackbusch and T. Probst. Downwind Gauss-Seidel smoothing for convection dominated problems. *Numer. Lin. Alg. Appl.*, 4:85–102, 1997.

[14] T. Hughes and A. Brooks. Streamline-upwind Petrov-Galerkin formulations for convection dominated flows with particular emphasis on the incompressible Navier-Stokes equations. *Methd Appl. Mech. Engng*, 32:199–259, 1982.

[15] A. Jameson. Solution of the Euler equations for two dimensional transonic flow by a multigrid method. *Appl. Math. Comp.*, 13:327–355, 1983.

[16] A. Jameson. Computational transonics. *Comm. Pure Appl. Math.*, 41:507–549, 1988.

[17] D. C. Jespersen. A time-accurate multiple-grid algorithm. AIAA paper 85-1493-CP, 1985.

[18] K. Johannsen. Robust smoothers for convection-diffusion problems with closed characteristics. *Computing*, 65:203–225, 2000.

[19] R. LeVeque. *Numerical Methods for Conservation Laws.* Birkhäuser, Zürich, 1992.

[20] K. W. Morton. *Numerical Solution of Convection-Diffusion Problems.* Chapman & Hall, London, 1996.

[21] R. H. Ni. A multiple-grid scheme for solving the Euler equations. *AIAA*, 20:1565–1571, 1982.

[22] C. W. Oosterlee, F. J. Gaspar, T. Washio, and R. Wienands. Multigrid line smoothers for high order upwind discretization of convection-dominated problems. *J. Comp. Phys.*, 139:274–307, 1998.

[23] A. Reusken. Multigrid with matrix-dependent transfer operators for a singular perturbation problem. *Computing*, 50:199–211, 1993.

[24] U. Trottenbery, C. Oosterlee, and A. Schüller. *Multigrid.* Academic Press, 2001.

[25] W. L. Wan and T. F. Chan. A phase error analysis of multigrid methods for hyperbolic equations. *SIAM J. Sci. Comput.*, 25:857–880, 2003.

[26] W. L. Wan, T. F. Chan, and B. Smith. An energy-minimizing interpolation for robust multigrid. *SIAM J. Sci. Comput.*, 21:1632–1649, 2000.

[27] F. Wang and J. Xu. A crosswind block iterative method for convection-dominated problems. *SIAM J. Sci. Comput.*, 21:620–645, 1999.

[28] P. Wesseling. *An Introduction to Multigrid Methods.* Wiley, Chichester, 1992.

[29] G. Wittum. On the robustness of ILU smoothing. *SIAM J. Sci. Stat. Comput.*, 10:699–717,

1989.

[30] I. Yavneh. Coarse-grid correction for nonelliptic and singular perturbation problems. *SIAM J. Sci. Comput.*, 19:1682–1699, 1998.

[31] I. Yavneh, C. H. Venner, and A. Brandt. Fast multigrid solution of the advection problem with closed characteristics. *SIAM J. Sci. Comput.*, 19:111–125, 1998.

[32] P. M. De Zeeuw. Matrix-dependent prolongations and restrictions in a blackbox multigrid solver. *J. Comp. Appl. Math.*, 33:1–27, 1990.

[33] P. M. De Zeeuw and E. J. Van Asselt. The convergence rate of multi-level algorithms applied to the convection-diffusion equations. *SIAM J. Sci. Stat. Comput.*, 6:492–503, 1985.

[34] R. Zvan, P. A. Forsyth, and K. R. Vetzel. Robust numerical methods for PDE models of Asian options. *J. Comp. Finance*, 1:39–78, 1998.